PCCP

Cite this: *Phys. Chem. Chem. Phys.*, 2011, **13**, 21035–21044

www.rsc.org/pccp

PAPER

A new form of spontaneously polarized material

Oksana Plekan,[a] Andrew Cassidy,[a] Richard Balog,[a] Nykola C. Jones[b] and David Field*[a]

Received 15th July 2011, Accepted 13th September 2011
DOI: 10.1039/c1cp22310k

We report here the discovery of a new form of spontaneously polarized material. Examples of this material, in the form of films, demonstrate the property that they spontaneously harbour electric fields which may exceed 10^8 Vm^{-1}, achieving potentials of tens of volts on the film surface. The molecules presently identified form a diverse group, thus far of six species, with gas phase dipoles lying between 0.08 D and 0.5 D: propane (0.08 D), isopentane (0.13 D), nitrous oxide (0.167 D), isoprene (0.25 D), toluene (0.385 D) and CF_3Cl (Freon-13; 0.5 D). Here we concentrate on an understanding of the nature of the interactions which give rise to the spontaneously polarized state, using the measured temperature dependence of the electric field in N_2O as a diagnostic. We show that the polarized state can arise through a mechanism of non-linear dipole alignment in a single domain in which dipole alignment generates the electric field within the film and the field generates dipole alignment. Non-local interactions take place over the dimension of the thickness of the film and permeate the entire medium through the agency of the electric field. This new type of material may have wide ranging applications in devices and in nanotechnology.

1 Introduction

A recent publication[1] reported the discovery that very substantial electric fields form spontaneously within thin films of nitrous oxide (N_2O) deposited on polycrystalline gold. Electric fields exceed $\sim 10^8$ Vm^{-1} for films laid down at 38 K. This finding, which is observed through the spontaneous generation of substantial potentials at the surface-vacuum interface, was attributed to dipole alignment between molecules in the film. This attribution appeared plausible but no clear demonstration was furnished. Here we report much more extensive studies of this phenomenon, giving insight into how the phenomenon comes about and placing it on a much broader footing than in ref. 1.

There are numerous classes of materials known to show spontaneous order giving rise to non-local electric fields. Examples, quite distinct from the present, are the creation of net polarization in individual domains in ferroelectric crystals,[2] in liquid crystals[3] and dipolar fluids,[4] the permanent electric dipole moments which have been observed in a variety of metal clusters[5] and electro-optically active materials. The latter for example may involve materials in the form of single crystals, generally of large organic species and polymers, showing long range acentric order stemming in part from electrostatic interactions.[6] Perhaps the most closely related phenomenon to that described here may be found in Kelvin probe measurements[7] of a potential as high as +28 V recorded on the surface of a room temperature 560 nm thick layer of the organic semi-conductor Alq_3 on gold, noting that some doubts appear to have been cast subsequently on aspects of these data.[8] Results in ref. 7 were attributed to dipole alignment suggesting $\sim$ 1% alignment in this species whose isomeric forms have dipole moments of 4.1 D and 7.1 D.

Data in ref. 1 raised a number of significant questions which are addressed here. These questions may be summarized as follows. (i) What is the nature of the interactions which give rise to the observation of a powerful electric field within the medium and how could these interactions be investigated experimentally? (ii) Is N_2O alone in showing this property or is there a class of compounds which show spontaneous polarization of which solid N_2O is but one member? (iii) Is the nature of the substrate of significance for the phenomenon to occur and, if so, does the nature of the substrate influence the magnitude of the electric field within the film? (iv) The highest voltage earlier recorded[1] was 4.8V. Could films maintain potentials which were significantly in excess of this value?

The work presented here concerns the electrical properties of spontaneously polarized material in relation to temperature of film deposition, film thickness and permanent dipole of the parent species. We consider in detail the first question posed above relating to the fundamental origin of the observed spontaneous polarization. We restrict ourselves to species in which the leading long range term in the intermolecular

[a] *Department of Physics and Astronomy, Aarhus University, DK-8000 Aarhus C, Denmark*
[b] *Department of Physics and Astronomy and Institute for Storage Ring Facilities (ISA), Aarhus University, DK-8000 Aarhus C, Denmark*

interactions is dipole–dipole, excluding species which exhibit hydrogen bonding, save briefly in the concluding comments.

Taking the questions in the order in which they are framed above, to investigate the origin of the electric field within the medium we propose that the structure of films is governed by a tendency to order through intermolecular forces, in particular dipole–dipole, where this tendency is countered by thermal motions. We report a detailed series of experiments on N_2O films, laying down layers of material at ten different temperatures. The electric field in the N_2O film is found to decrease rapidly with temperature and this variation may be reproduced with a simple parameterised theory of the Langevin-Debye type. Results are found to support the dipole induced order *vs.* thermal disorder model. The answer to the second question: is N_2O alone? is firmly in the negative. Between the range of dipoles 0.08 D (for propane) to 0.5 D (for trifluorochloromethane, CF_3Cl) all films tested show spontaneous polarization behaviour for a range of chemically diverse species. The answer to the third question, with regard to the nature of the substrate, is that the identity of the substrate has no influence within experimental accuracy of a few meV on the magnitude of the electric field generated within the medium. This emphasises the generality of the phenomenon whose discovery is reported here.

It is well-known that the adsorption of a monolayer of atoms or molecules on surfaces creates a surface dipole layer.[9] This gives rise to surface potentials, of either sign, typically of a few hundred meV and contributes to work function change on monolayer adsorption. The adsorption of further layers does not change the apparent work function markedly, that is, there is no additional change in the surface potential after several layers are added. Thus the observations reported here and in ref. 1 are anomalous in that potentials at the surface-vacuum interface of adsorbed species continuously increase with film thickness.

In section 2 below we describe the experimental technique used to measure potentials on the surface of films. In section 3, detailed measurements are presented for electric fields within films of N_2O involving data for ten film deposition temperatures between 38 K and 65 K. In section 4 we outline the properties of films of propane, isoprene, toluene, isopentane, CF_3Cl and some composite films. In section 5 we present a phenomenological model, mentioned above, which addresses the temperature dependence of electric fields in films with particular reference to N_2O data, with a view to understanding the physical mechanism which underlies the results described here. In section 6 we consider the insight into the nature of the spontaneously polarized films that may be gained from the lack of dependence of the properties of the film on the identity of the substrate. In section 7 we briefly describe how heterostructures may be formed, giving an example of a quantum well.

2 Experimental method

2.1 The apparatus

The potentials on film surfaces are measured, as described in ref. 1, by interrogating the surface with electron beams of lowest energy of 2–3 meV and maximum current typically of 200 fA. The essential elements of the apparatus are shown in Fig. 1. Electrons are generated in a cell at a nominal zero potential through

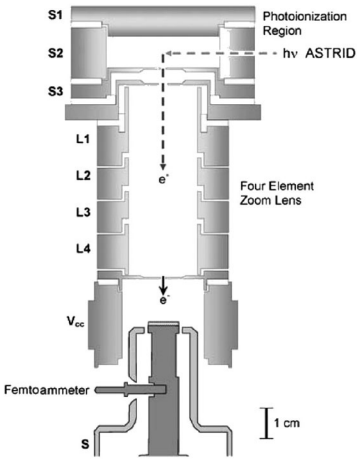

Fig. 1 A scale diagram of the UHV apparatus. Synchrotron radiation (hν ASTRID) with a resolution of 1.5 meV enters a photoionization source S1, S2, S3 containing argon at a pressure of typically 10^{-4} mbar. Photoelectrons are transported onto condensed solid films at temperatures of 38 K and above. Currents are detected with a Keithley 6340 femtoammeter.

photoionization of Ar within ~ 5 meV of threshold (78.67 nm or 15.764 eV) at the $3p^5(^2P_{3/2})9d$ resonance (78.675 nm ~ 15.759 eV). This is performed using focussed synchrotron radiation of resolution ~ 1.5 meV from the ASTRID storage ring at Aarhus University,[10,11] where all experiments described here were performed. This creates photoelectrons with a corresponding energy resolution of ~ 1.5 meV. The photon beam waist is a few tens of microns and electrons are expelled from the region of photoionization in a 0.4 Vcm^{-1} electric field without significant loss of energy resolution.[11] The beam of electrons so formed is transported through a 4-element electrostatic lens, L1–L4 (Fig. 1) and impinges on the film surface.

2.2 Substrate, cooling and film preparation

The base pressure of the system is ~ 10^{-10} mbar. When performing experiments to measure surface potentials the total pressure rises to ~ 10^{-7} mbar when Ar is introduced into the photoionization region. The gas is of 99.9999% purity and investigations show no evidence of deposition of impurities onto the gold substrate or of molecular films arising from many hours exposure to this pressure of Ar. In addition, without Ar present, surface contamination from background gas or charging of films in the absence of an electron beam could not be detected. A very sensitive check of this is the stability at the mV level of the surface potential of the gold or of a molecular film, noting that any accumulation of impurities or some source of charge would lead to a readily detectable effect. Experiments on the charging of ice[12] have established that changes in potential at the sample of 1 to 2 meV may be detected with this system.

Films are prepared under UHV conditions and are laid down on a polycrystalline Au substrate, grain size < 100 nm, in the form of a 750 nm thick layer of material on Ta. The substrate is cooled with a He cryo-cooler to temperatures in the range of 38 K upwards and cleaned by heating to 750 K. Standard dosing techniques from the background gas allow the deposition of uniform films of a known number of monolayers (ML)

using temperature programmed desorption (TPD), where 1 ML is $\sim 10^{15}$ molecules cm^{-2}. The rate of dosing differed substantially from one species to another varying between 0.4 ML min^{-1} for isoprene to 10.7 ML min^{-1} for CF_3Cl normalised to the same background dosing pressure of 5×10^{-8} mbar. Dosing rates were measured to be independent of the temperature at which dosing was performed, that is, the deposition temperature, for the ranges of temperature of interest here. Note that absolute numbers of ML are known to no better than $\pm$ 20%. Relative values are however accurate at the few percent level.

The molecules investigated are not found to decompose on the polycrystalline gold surface at the temperatures employed. TPD data show no trace of any species other than the pure gas with which the surface was dosed. This is in keeping for example with results reported for N_2O on Ag.[13]

2.3 The principle of measurement of surface potentials

Since electrons are formed at nominally zero volts with an energy of $\sim$ 5 meV, the beam should therefore just be able to reach a target when the target is itself at this same nominal zero. If the surface of the target were not at zero but rather, say, at +5 volts due to spontaneous formation of an electric field within the film, then in order to ensure that the electrons only just reach the target it would be necessary to bias the target 5 volts negative. Measurement of the bias required to locate the onset of a measurable current, that is, 1 to 2 femtoamps, therefore gives the potential on the surface of the film. There is a small correction to be made to establish a true zero difference between the clean gold substrate and the potential of formation of the electrons. This arises from the difference between the work function of the gold substrate and the graphite walls of the photoionization chamber in which electrons are formed, labelled S1, S2 and S3 in Fig. 1. We have measured a value of $\sim$ 0.25 V in agreement with standard values. All recorded values of surface potential are with respect to the clean Au substrate.

A crucial difference between the present experiments and earlier work relating to electron irradiation of molecular films, save ref. 12, is that here the dose of electrons is two to three orders of magnitude lower.[14] Thus we interrogate the material while perturbing it to a minimum, in particular by the avoidance of strong charging. We return to this point in more detail in section 4.

2.4 Use of a trochoidal electron monochromator (TEM)

In addition to experiments using the Ar synchrotron radiation source described above, experiments have also been performed using a TEM,[15] the principle of operation of which has most recently been reviewed in ref. 16. Very briefly, energy selection operates through the electron energy dependence of the physical displacement of an electron beam, generated from a filament, in a crossed E-B field. Our TEM, not shown in Fig. 1, is a miniaturised version which is fitted before the element S1 of the photoionization source. This has a 1.8 mm diameter aperture at its centre to allow the passage of electrons from the TEM. The TEM employs an axial magnetic field of $\sim 10^{-3}$ T in our system and the resolution in the beam is estimated from the current onset to be $\sim$ 150 meV. The energy onset of current detection is then determined by the potential of the filament relative to that of the gold substrate.

The TEM enables us to locate current onsets to better than 10 mV, given the high stability with which we are able to run the source at currents of 200 fA and below. The TEM provides a valuable 'quick look' at films and also allows us to use high currents, for example several picoamps, to observe the removal of the surface potential by electron trapping (see section 4).

3 Electric fields in nitrous oxide films

Our hypothesis is that potentials on the surface of molecular films and the associated electric fields within films are generated through the cooperative dipole alignment of individual species of which the films are composed. Thus dipole alignment is proposed to give rise to a non-zero surface polarization. At the surface-vacuum interface the positive or negative end of the molecule may essentially protrude from the surface giving rise to surface polarization and generating an electric field within the film. In the case of N_2O, the positive nitrogen moiety of N_2O protrudes at the surface-vacuum interface and the resulting charge density on the surface gives rise to a positive voltage.

The very low currents used to measure the surface potential ensure that negligible charge is trapped within the film. Gauss's theorem then requires that the electric field within the film be constant. Thus the surface potential should increase linearly with layer thickness with an intercept equal to the work function change of Au associated with a monolayer addition,[9] here of the order of $\sim$ 200 mV at 40 K. A linear relationship of the surface potential with layer thickness was observed for N_2O, for all layers of $>$30 ML.[1]

Fig. 2 shows data for the variation of the surface potential on N_2O as a function of film thickness for a set of ten different films each corresponding to a different deposition temperature. These lie between 38 K and 65 K, the latter temperature a few degrees below the maximum temperature at which N_2O can be deposited on polycrystalline Au. Films were accumulated through successive depositions of 71 ML. Random errors in potentials are 2–3 meV. Some systematic errors arise through

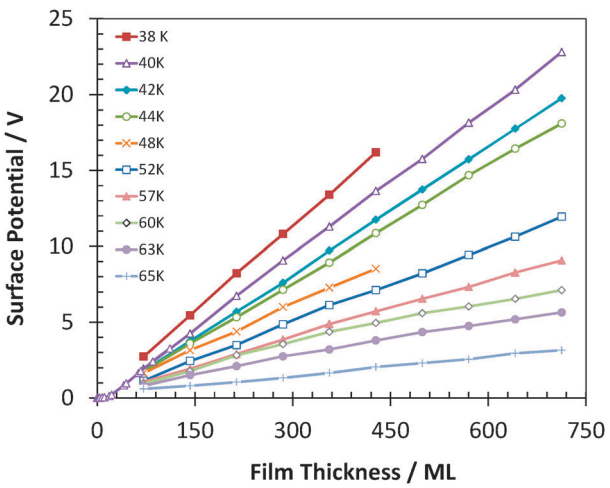

Fig. 2 Surface potentials measured for films of N_2O as a function of thickness in monolayers (ML) laid down at ten different deposition temperatures. Data at 40 K from ref. 1 have been included for films of thickness $<$ 71 ML.

small variations in the film temperature of ± 0.25 K between depositions over the typical duration of an experiment of about 90 min for any one temperature. With regard to data at 40 K for ilms of < 71 ML taken from ref. 1 and shown in Fig. 2, the number of monolayers was overestimated by ~ 35% in that work due to an accumulation of errors in calibration. This has been corrected here. In addition temperature measurement techniques have been considerably refined in the present work.

Fig. 3 shows the corresponding electric fields, E_{obs}, in films of N_2O. Observed electric fields are also tabulated in Table 1. Values of E_{obs} are the measured surface potentials divided by film thicknesses, the latter given by the number of ML times a layer spacing s = 0.32 nm between successive N_2O layers. Data obtained with the TEM, for example for N_2O films of 71, 142, 213 and 355 ML at 40 K, match those shown in Fig. 2 within a few mV demonstrating that there are no unrecognized artefacts associated with use of the more unconventional high resolution photoionization source.

Electric fields achieve values of > 10^8 Vm^{-1} at 38 K. In this connection for solids in general, breakdown fields[17] vary between 10^8 Vm^{-1} to 10^9 Vm^{-1}, where electromechanical stress is induced by elastic deformation and electron cascade.

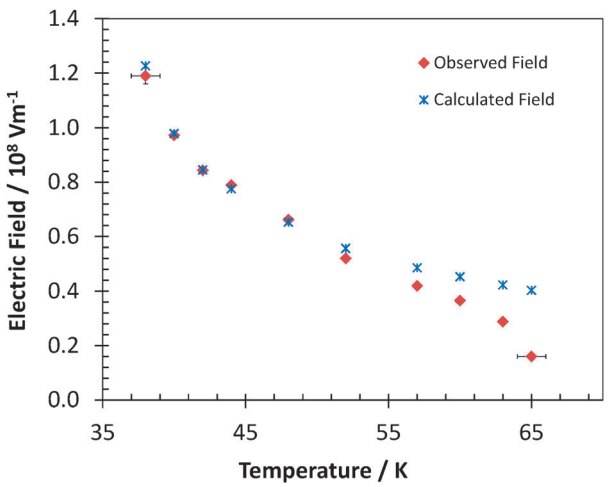

Fig. 3 Observed electric fields in N_2O (red diamonds) and calculated values (blue crosses) as a function of the temperature at which films of N_2O were laid down.

Table 1 Data for N_2O: observed electric fields and the corresponding degree of dipole alignment $\langle\mu_z\rangle/\mu$ obtained from data shown in Fig. 2 and 3 for a set of deposition temperatures T. Also shown are the electric fields and values of $\langle\mu_z\rangle/\mu$ obtained from the mean field theory describe in section 5

T/K	Obs. field/Vm^{-1}	Calc. field/Vm^{-1}	$\langle\mu_z\rangle/\mu$ from observations	$\langle\mu_z\rangle/\mu$ calculated
38	1.189×10^8	1.227×10^8	0.1520	0.1552
40	9.723×10^7	9.783×10^7	0.1242	0.1238
42	8.436×10^7	8.448×10^7	0.1078	0.1069
44	7.889×10^7	7.754×10^7	0.1008	0.0981
48	6.616×10^7	6.529×10^7	0.0846	0.0826
52	5.205×10^7	5.567×10^7	0.0665	0.0704
57	4.196×10^7	4.859×10^7	0.0536	0.0615
60	3.655×10^7	4.530×10^7	0.0467	0.0573
63	2.882×10^7	4.228×10^7	0.0368	0.0535
65	1.598×10^7	4.034×10^7	0.0204	0.0510

The latter will be inhibited by inelastic scattering of electrons within solid films.

Using N_2O films we have also addressed specific questions set out in the introduction. First, is the nature of the substrate of significance for the phenomenon to occur and, if so, does the nature of the substrate influence the magnitude of the electric field within the film? Second, can films maintain potentials which were significantly in excess of the highest voltage of 4.8 V earlier recorded in a previous publication?[1]

In order to address the first question, four films have been prepared of Xe of 1 ML and 50 ML at 58 K, 15 ML at 63 K and 5 ML at 65 K with N_2O deposited over the Xe in each case at the same temperature as the Xe deposition. No significant difference at the mV level was found for the value of the electric field within N_2O films compared with pure N_2O films laid down at these temperatures. The conclusion is that the identity of the substrate has no influence within experimental accuracy of a few mV on the magnitude of the electric field generated within the medium. This conclusion is discussed in section 6 and reinforced by experiments involving other composite hetero-structures films, reported in section 7.

The answer to the second question, regarding the limit of potential that can be achieved, is that a potential as high as 38 V has been measured at the surface-vacuum interface for films of N_2O of 1250 ML at 40 K. Numerous other examples of high potentials are illustrated in Fig. 2. Since we float the femtoammeter to the surface potential, the maximum measurable potential is essentially limited only by the electrical integrity of the measurement devices involved.

4 Electrical properties of other films

As mentioned in the introduction, the phenomenon reported appears widespread, at any rate for low dipole moment species. Here we briefly consider each of the species investigated: propane, isoprene [CH_2═$C(CH_3)CH$═CH_2], toluene, isopentane [$CH_3CH_2CH(CH_3)_2$], CF_3Cl (Freon-13) separately. Structures of these species are shown for reference in Fig. 4 which also underlines the diversity of their form.

Isoprene and toluene show positive potentials on their surface, whereas CF_3Cl, isopentane and propane show negative potentials. All species show strong temperature dependence of the potential and relevant data are shown in Fig. 5–9 respectively. Propane is discussed separately. Any deviations in linearity in

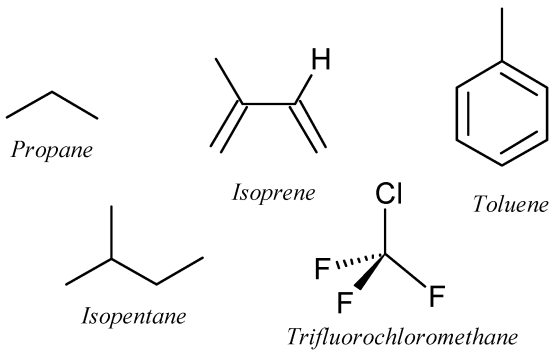

Fig. 4 Structures of the molecules investigated, other than N_2O, which show spontaneous polarization.

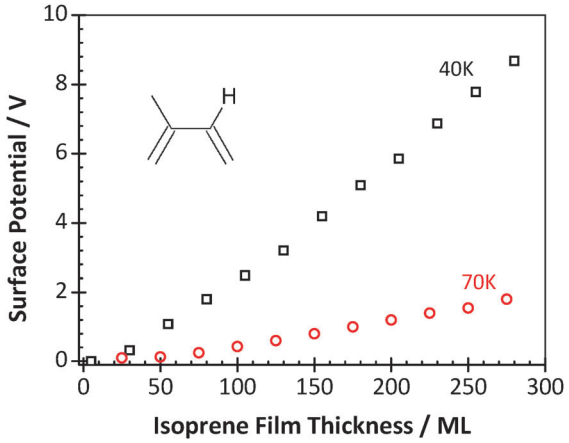

Fig. 5 The variation of the surface potential on films of isoprene at 40 K and 70 K.

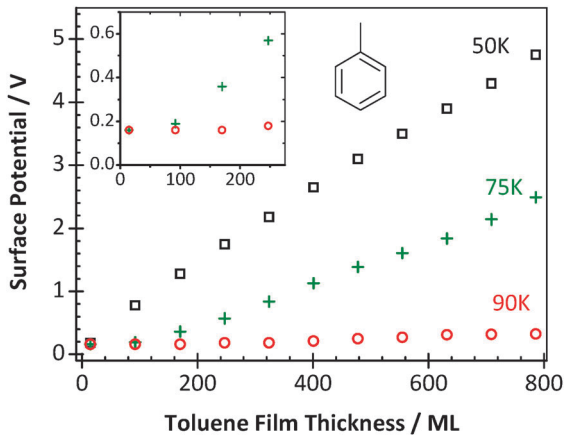

Fig. 6 The variation of the surface potential on films of toluene at 50 K, 75 K and 90 K. The inset shows the behaviour at low coverage for 75 K and 90 K.

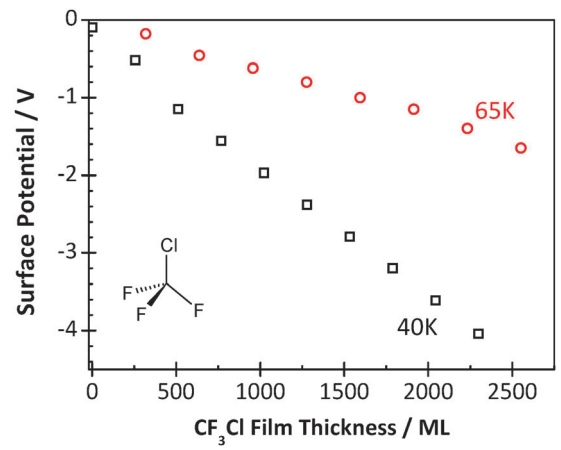

Fig. 7 The variation of the surface potential on films of CF_3Cl at 40 K and 65 K.

data above some critical layer thickness arise from lack of precise control of the deposition rate as successive layers were added. Electric fields associated with each species for deposition at 40 K

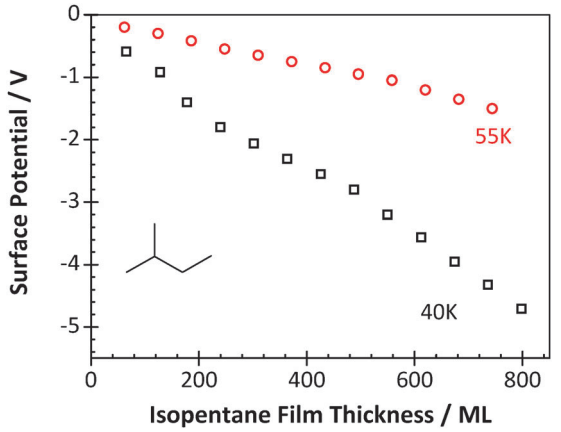

Fig. 8 The variation of the surface potential on films of isopentane at 40 K and 55 K.

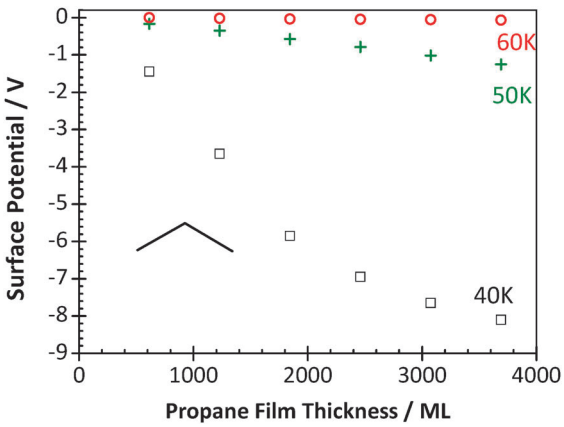

Fig. 9 The variation of the surface potential on films of propane in phase 1 at 40 K, 50 K and 60 K.

are collected in Table 2. These are expressed as mV per ML added rather than Vm^{-1} since we do not have well-established values of the layer separation in these solids. Note subsequent comments below on small systematic effects of charging and the errors associated with this.

A particular characteristic of spontaneously aligned material in general is that a temperature may be encountered at which the polarization alignment and therefore, in our case, the surface potential disappears as the material is heated. Material is meanwhile not evaporated from the surface and the film survives but is no longer aligned. Isoprene, isopentane and toluene all show this behaviour, which is the equivalent of the existence of a Curie temperature in ferromagnetism or the loss of spontaneous

Table 2 Observed electric fields, expressed as mV per ML added, for layers of molecules deposited at 40 K

Molecule	mV ML^{-1}	Dipole Moment /D
Propane	−0.72 and −4.77	0.08
Isopentane	−7.8	0.13
Nitrous oxide	+32	0.167
Isoprene	+35	0.25
Toluene	+6	0.385
Trifluorochloromethane	−1.7	0.5

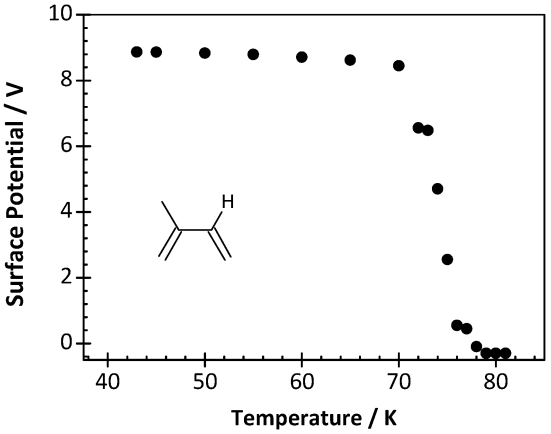

Fig. 10 The variation of the surface potential of a 300 ML film of isoprene laid down at 40 K and warmed to 82 K showing a Curie point.

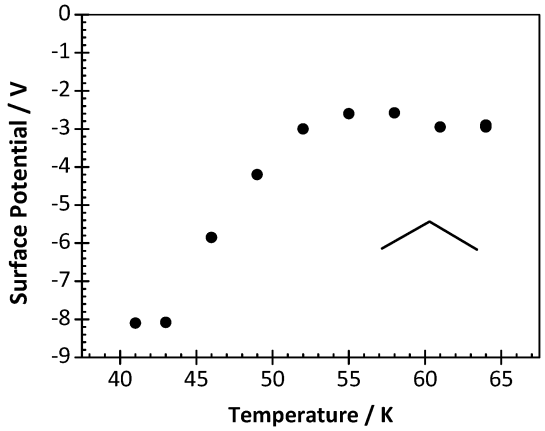

Fig. 11 The variation of the surface potential of a 3700 ML film of propane laid down at 40 K and warmed to 65 K.

polarization in piezoelectric materials. The example of isoprene is given in Fig. 10. The film was warmed from 40 K to 82 K over a period of 160 min showing an abrupt change in potential around 70 K terminating at 80 K. The final potential of the film surface relative to the gold surface is −0.3 V at > 80 K, a small but interesting effect for which we have no explanation at present. Note that isoprene begins to evaporate from the gold substrate only above 105 K.

The analogy with ferromagnetism is incomplete since on cooling from above the critical temperature to 38 K, our lower limit, isoprene, isopentane and toluene have not been found to re-establish any surface potential. Thus the effect is not demonstrably reversible. The material appears locked into an energetically unfavourable state from which it cannot stray, at any rate on a timescale of hours. Curie-like behaviour cannot be clearly identified in nitrous oxide and CF_3Cl since the temperature of evaporation and the sudden decay of surface potential are located at effectively the same temperature.

Preliminary data on propane, with a gas phase dipole moment of 0.08 D, show that this species is alone in this group of molecules in showing evidence of the formation of two phases. One phase yields −4.77 mV ML^{-1} (phase 1) and the other −0.72 mV ML^{-1} (phase 2) at 40 K. The rate of propane deposition appears to determine which phase forms. Phase 1 shows a strong temperature dependence of the field as shown in Fig. 9, noting that the material may be in phase 2 for the 60 K data. A 3700 ML layer of phase 1 on warming between 41 K and 65 K, over a period of 120 min, demonstrates a clear Curie-like behaviour between 45 K and 52 K, becoming abruptly less negative over this temperature range as shown in Fig. 11. However a potential of ∼−3 V survives, suggesting a change to phase 2, which on the basis of the above figure of −0.72 mV ML^{-1} would yield ∼−2.66 V. Phase 2 has been observed to show dipole alignment up to deposition temperatures of 70 K. Preliminary experiments with warming to close to the Curie temperature and subsequent cooling appear to give rise to more classical hysteresis behaviour. The case of propane is evidently rather complex and requires further experiment.

Materials may in general charge negative on irradiation by electron beams[18] introducing systematic errors into our data. The extent of charging may be measured by repeated scanning of the electron current as a function of potential for any chosen film thickness and observing any shift in the onset. Such a shift would represent the accumulation of a negative potential and introduce errors into the data. No effect of charging is observed for N_2O, propane or isoprene at the level of < 2 meV for 100 s of irradiation at 200 fA over an incident electron energy range of zero to 500 meV. For propane we estimate that charging leads to an overestimate of negative values shown in Table 2 by ∼ 5% in the case of the lower figure of −0.72 mV ML^{-1} and < 1% for the figure of −4.77 mV ML^{-1}. The error for films of toluene, which charges appreciably, lead to an underestimate by 9% and a better estimate than that in Table 2 may be therefore 6.5 mV ML^{-1}. For CF_3Cl charging yields an overestimate of 2%.

5 An electrostatic model

The purpose of this section is to develop an understanding of the physics at play in creating the potentials which we observe on the surface of thin films and in forming the associated electric fields within these films. The analysis presented here has the limited objective of reproducing the variation of surface potentials and electric fields with temperature shown in Fig. 2 and 3 for N_2O. For the present, phase transitions or any form of critical behaviour, either involving different polarized phases or at the Curie temperature, are not considered. The hypothesis which we seek to test is that the mechanism for the creation of electric fields in the film is due to a tendency of the molecular dipoles to align in successive layers of the material, a tendency countered by thermal motion.

At the surface-vacuum interface, the protrusion of the positive moiety of N_2O results in a charge density on the surface and gives rise to polarization and a positive voltage. Equally, the more negative end of isopentane (for example) protrudes from the surface giving a negative surface potential. The only net charge introduced into the film is that from the electron beam, which was shown experimentally in ref. 1 to be insignificant in reducing the potential on the surface of N_2O and, as discussed at the end of section 4, has either small or no effect on any of the species studied here and no measurable effect on N_2O for the very low currents used. At 40 K the value of the polarization[1] is ∼ 1.1×10^{-3} Cm^{-2}. The diameter of the sample irradiated is

6 mm and the polarization charge is therefore $\sim 1.2 \times 10^{11}$ charges. The fluence of electrons by comparison is 200 fA for 100 s $= 1.25 \times 10^{8}$ charges, illustrating why the electron beam has no influence on the measured potential. This conclusion is borne out by the constancy of the electric field within N_2O films. In the model outlined below, polarization resulting from dipole alignment gives rise to the electric field and free charges are assumed to make no significant contribution.

In this connection we have performed experiments using the TEM (section 2.4) to irradiate a 355 ML sample of N_2O laid down at 60 K with $\sim$ 13 pA for a total of 45 min, equivalent to a fluence of 2×10^{11} charges. The initial polarization potential of 3 V, representing in this case a polarization equivalent to 4.6×10^{10} charges, was completely removed. This and other results with the TEM offer an explanation of why the phenomenon of spontaneous polarization has not been observed in numerous earlier experiments of other groups in which currents were generally nA and times of irradiation a few to tens of seconds.[19]

There is a host of theoretical work devoted to phenomena for both ferromagnetic and ferroelectric materials, with which the present polarized phase has aspects in common, based on Ising lattice models.[20] Lattice systems in which electric moment interactions play a fundamental role are treated for example in ref. 21. In common with this and much other work a lattice model is adopted here using a Hamiltonian which is composed of a long range dipole–dipole interaction and a term which essentially frustrates the attempt of the dipoles to align. In addition and in contrast to much other theory, a non-linear, non-local interaction is included which represents the energy associated with the interaction of the electric field created through dipole alignment with the dipoles themselves. The system is non-linear and non-local since alignment of dipoles creates the field and the field itself creates dipole alignment. Thus all components of the film communicate over all ranges. The film, in the absence of barriers, settles down to a stable configuration corresponding to a balance between the non-linearity which leads to order and thermal motion which leads to disorder. This concept of dipole–dipole ordering countered by a tendency to disorder through thermal motion follows naturally from the strong temperature dependence of the electric field on deposition temperature, illustrated in Fig. 3. The control parameter of the physics is therefore the energy associated with the interaction of the dipole with the local electric field divided by the thermal energy.

This non-linear order-disorder problem may be solved by methods set out by Langevin, Debye and Landau, using so-called mean field theory. Solutions yield the average direction in which a dipole is pointing within the film, relative, say, to the normal to the film surface, as a function of temperature. This in turn gives the amount of polarization charge at the surface-vacuum interface per unit area – the polarization – and hence the electric field within the material. Values emerging from the model are fitted to observed data of electric field *versus* temperature, using three temperature-independent parameters described below and yielding results shown as blue crosses in Fig. 3. The good agreement between this theory – albeit parameterized – and observations gives strong support to the hypothesis that dipole alignment is the cause of the unexpected electrical nature of the films reported here. Note also that dipoles are not pointing vertically but rather are typically aligned at an angle of more than 80° to the normal. The formulation of the theory is outlined below.

Values of E_{obs}, the observed electric field in the film, given in section 3 as a function of deposition temperature, provide the spatially averaged value of the dipole moment in a direction normal to the surface, $\langle \mu_z \rangle$ as a function of temperature. We refer to $\langle \mu_z \rangle / \mu$ as the degree of dipole alignment, where μ is the total moment of N_2O in the solid environment and $\langle \mu_z \rangle / \mu$ is equal to the cosine of the average angle, θ, between the direction of μ_z and μ. The degree of dipole alignment is derived from E_{obs} as follows. First we record that components E_x and E_y in the xy-plane of the substrate surface are identically zero on average; there are on average as many species with dipoles pointing one way as the other in the surface plane. The macroscopic polarization may be expressed as $P_{obs} = \varepsilon_0 E_{obs}$, noting the absence of a permittivity for reasons to be given below. P_{obs} is the effective charge/unit area which may be equated[7] with the component $\langle \mu_z \rangle$ divided by the volume of the molecule, Ω. Thus $E_{obs} = [\langle \mu_z \rangle / \Omega] / \varepsilon_0$ or $\langle \mu_z \rangle / \mu = \varepsilon_0 E_{obs} \Omega / \mu$, giving the degree of dipole alignment from the observed field.

The value of the dipole moment, μ, in the solid environment in the above expression for $\langle \mu_z \rangle / \mu$ is reduced by depolarization[22,23] from the gas phase value, μ_0, to a value given by $\mu = \mu_0 / (1 + \alpha k / s^3)$. Here α is the polarizability and has the value 3.31×10^{-30} m^3 for N_2O and s is the layer spacing $= 0.32$ nm as earlier. Since we use a depolarized value of μ, this simulates the response of the medium to an applied field and effectively introduces a local field correction. Thus a static permittivity does not figure above. The value of k depends on the geometry[23] and we choose $k = 11.034$ giving $\mu = 0.0785$ D which may be compared with the gas phase value of 0.166 D. The molecular volume, Ω, has been estimated using the value of polar surface area for N_2O of 56.46 Å^2 yielding $\Omega = 3.779 \times 10^{-29}$ m^3. Values of the degree of dipole alignment are shown in Table 1 and vary between 2% at the highest temperatures to 15% at the lowest.

In the current model the forces in solid N_2O are simulated through an electric field acting on a dipole, where this electric field represents both the origin of the familiar forces which bind N_2O molecules to form films and the electric field, created by the oriented dipoles, which permeates the film. The electric fields which represent interactions which bind one layer to the next are backward-forward symmetric and those from dipole alignment are asymmetric in the direction normal to the film. Backward-forward symmetric interactions, represented by E_{sym}, include those that bind one layer of adsorbed material to the next, be it dipolar or not, the latter as in Xe films, say. These interactions give rise to zero net electric field in the medium. The asymmetric interactions, E_{asym}, are the end-to-end dipole interactions, that is, the μ_z^i with μ_z^{i+1} interactions, where i and $i + 1$ refer to successive layers. These interactions give rise to dipole ordering and create the measured electric field in the film, E_{obs}. We use a mean field (or Landau) model which makes no spatial distinctions. The presence of the metal-adsorbate interface and an adsorbate-vacuum interface however breaks the symmetry. This allows us to define a z-direction normal to the surface and thus an asymmetric field in the z-direction.

The influence of the substrate surface must be such that in the case of N_2O the majority of species are physisorbed with their negative (oxygen) ends towards the substrate surface,[24] whereas in (say) CF_3Cl the positive moiety points towards the substrate surface.

The change in work function associated with adsorption of a monolayer[9] may be represented by an electric field created by the substrate forming a surface dipole. For species which show spontaneous polarization, the field must be sufficiently strong to overcome the propensity of dipoles in the first monolayer to line up side-by-side, $\delta+$ to $\delta-$, which if strongly dominant would result in very little net effective surface charge as subsequent layers are added. In passing, this may be the origin of an apparent optimum dipole moment for dipole alignment, around 0.25 D (Table 2), rather than a general increase in the alignment with increasing dipole moment, differences in depolarization of the gas phase dipole in the solid environment apart. In support of this hypothesis we find that carbonyl sulphide, OCS, deposited at 40 K, does not form a spontaneously polarized film where OCS has a dipole moment of 0.7 D. We note that while this explanation may suggest an optimum dipole it does not give any quantitative insight into why the optimal value should lie around 0.25 D or indeed that it is only the dipole moment which dictates the observed behaviour. This must await sophisticated computational models, as further comments in the conclusion, section 8, emphasize.

In a manner analogous to the derivation of Curie's law for paramagnetism, we proceed by invoking a thermodynamic balance between the mean interaction energy of the dipole with the local electric field, E_z, and the thermal energy, kT, where T is the temperature at which the film was laid down; see eqn (1) and (2) below. The mean field approximation is embodied in the statement that the dipole in the ith layer, at some angle to the normal, may be equated to the average dipole at all sites and all angles. The backward-forward symmetric field, E_{sym}, includes contributions from anti-ferroelectric dipole–dipole forces, dipole-image charge forces and associated polarization interactions, all of which are involved in moderating thermal fluctuations of molecular motions. These symmetric interactions share the common feature that they have an angular dependence governed by $cos^2\theta$, that is by $(\langle\mu_z\rangle/\mu)^2$, a dependence which includes arrays of dipoles and extended dipoles.[25–27] The net local field experienced by an average dipole may be expressed as

$$E_z = \langle E_{sym}\rangle\left[1+\zeta\left(\frac{\langle\mu_z\rangle}{\mu}\right)^2\right] - \langle E_{asym}\rangle\frac{\langle\mu_z\rangle}{\mu} \qquad (1)$$

where the first term is the backward-forward symmetric field in the film and the second term the backward-forward asymmetric field created by the average dipoles and experienced by the average dipole. $\langle E_{sym}\rangle$, $\langle E_{asym}\rangle$ and ζ are temperature independent fitting parameters of the model designed to reproduce the variation of $\langle\mu_z\rangle/\mu$, and hence the theoretical electric field in the film, $\langle E_{asym}\rangle\langle\mu_z\rangle/\mu$, with deposition temperature. The energy of interaction of the average dipole is eqn (1) multiplied by μ.

On the basis of textbook analysis, the mean field theory yields an implicit equation for $\langle\mu_z\rangle/\mu$ involving the Langevin function $\coth(x) - 1/x$ where $x \equiv E_z\mu/kT$. Hence we seek solutions of the implicit equation

$$\frac{\langle\mu_z\rangle}{\mu} = \coth\left(\frac{E_z\mu}{kT}\right) - \left(\frac{E_z\mu}{kT}\right)^{-1} \qquad (2)$$

which combined with eqn (1) allows values of $\langle\mu_z\rangle/\mu$ and the electric field to be obtained numerically.

Fig. 3 shows the result of a fit obtained using data between 38 K and 57 K. Data at 60 K, 63 K and 65 K have been excluded from the fit since, at these temperatures, which approach evaporation, fluctuations in the local dipole orientation become large and mean field theory may not hold. Indeed values of $\langle\mu_z\rangle/\mu$ drop increasingly rapidly above 60 K. The parameters associated with the fit in Fig. 3 are $\langle E_{sym}\rangle = 5.43 \pm 0.2 \times 10^8$ Vm^{-1}, $\langle E_{asym}\rangle = 8.24 \pm 0.3 \times 10^8$ Vm^{-1} and $\zeta = 43.8 \pm 3.0$. For example at 40 K, the symmetric part of the field $= 1.27 \times 10^9$ Vm^{-1} and the asymmetric $= 1.02 \times 10^8$ Vm^{-1} using eqn (1) and the value of $\langle\mu_z\rangle/\mu$ of 0.1242 (Table 1). Thus at this temperature the symmetric contribution to the local field is approximately an order of magnitude larger than the asymmetric contribution.

Calculated values of $\langle\mu_z\rangle/\mu$ and the theoretical electric field, $\langle E_{asym}\rangle\langle\mu_z\rangle/\mu$, are shown in Table 1. The experimental values of the electric field due to dipole alignment, E_{obs}, are reproduced simultaneously with $\langle\mu_z\rangle/\mu$ to better than 10% for temperatures $\leq$ 52 K.

6 Implications of a lack of substrate effects

The above model ignores the nature of the substrate on which N_2O or other material is laid down, by implication requiring that potentials observed are independent of the nature of the substrate. Also implicit in the model is the assumption that the effective dipole moment of N_2O (say) is the value engendered through the N_2O environment without any substrate influence. Thus the model is only for bulk material and, within the confines of the model, the degree of dipole alignment should be independent of the nature of the substrate. This is corroborated by experiments involving Xe layers separating the gold substrate from N_2O as described in section 3. Further evidence is mentioned in section 7 in which a hetero-structure is introduced.

The conclusion that we are dealing with a bulk effect which depends to a very large degree only on the film gives insight into the nature of the phenomenon of macroscopic dipole alignment. An analogy may be made with a free running saturated non-linear system, for example a strongly saturated interstellar hydroxyl maser.[28] In such a non-local non-linear system all knowledge of the starting conditions are lost over a short physical extent compared with the total length (thickness) of the system. The system maintains a constant condition through almost its entire length and locks into a rigid configuration from which it may not be displaced without some major perturbation. This may be for example through heating represented by Curie temperature measurements in Fig. 10 and 11 and by additional data which we describe in the succeeding paragraph. By analogy with a saturated maser, gain is represented in the present case through the creation of electric field through dipole alignment and stimulated events through the electric field itself creating dipole alignment. Loss is through thermal motion which opposes dipole alignment as described in section 5.

So long as gain overcomes loss, the molecules self-organise losing memory of the initial state from which order emerged.

With regard to the rigidity of the system, the robustness of films to temperature stress has been tested. For example, for N_2O a film was laid down at 38 K and heated with measurements taken every 3–4 K to just below the evaporation point at 75 K. The surface potential was measured at each temperature. The potential dropped by only 510 meV at 75 K. This may be compared with data in Fig. 2 where results for the relaxed state show a drop of 11.95 V between 38 K and 65 K, where these temperatures refer to temperatures of film deposition. Evidently the dipole-aligned structure shows powerful rigidity and remains in place despite the substantial electromechanical stress that this implies. This may also be seen in the Curie point measurements shown in Fig. 10 for isoprene where the surface potential remains nearly constant up to 70 K whereas Fig. 5 shows that a drop of more than 6 V would be expected.

7 Fabrication of a heterostructure quantum well

We have tested the idea that it should be possible to tailor any set of potentials by combining films to form a heterostructure. In principle, for example, one might be able to combine films which possess a positive surface potential with those that possess a negative potential to create a quantum well. On the basis of experimental data for the individual species, it is known that at 40 K 33 ML of N_2O would give $+800$ mV and subsequent deposition of 183 ML of isopentane would give -800 mV, creating a net zero polarization potential on the surface and yielding an asymmetric triangular well of depth 800 meV. This is based on the assumption that there is no significant interpenetration of these two layers.

Remarkably this simple prescription worked exactly as described. A 33 ML film of N_2O was prepared forming a positive surface potential of 800 mV and as isopentane was dosed in stages on top of the N_2O the reduction of the 800 mV potential to zero could be followed, a value achieved when 183 ML of isoprene had been formed, just as predicted from the behaviour of the independent layers. A further layer of N_2O was added raising the potential once more to 800 mV with a subsequent layer of isopentane restoring the potential to zero. There was no necessity for, say, a Xe spacer between the two species and the development of the isopentane potential proceeded exactly as on deposition on polycrystalline Au, reinforcing comments in sections 3 and 6 referring to the independence of behaviour on the nature of the substrate. We infer that the interface between the N_2O and isopentane layers must be such that the negative O moiety of N_2O must line up with the positive end of the isopentane species.

8 Concluding remarks

The present work has shown that spontaneous dipole alignment is a general phenomenon in thin films of weakly dipolar species. However our results raise numerous questions. No quantitative explanation is furnished of why some surface potentials are positive and some are negative, why there is such a marked difference in efficacy of different species in creating surface potentials or what is the full range of dipoles over which spontaneous polarization may be observed. The value of the optimal dipole around 0.25 D has already been mentioned as a puzzle whose solution requires models based on detailed chemistry codes. As a further example our results suggest that the transition from spontaneously polarized to non-polarized behaviour occurs between 0.5 D and 0.7 D, the latter for OCS. One may ask, why these values? It is evident that sophisticated models are necessary to make convincing statements since the chemical details of the species involved as well as purely their dipole moments may play a significant role.

In addition, in recent experiments we have tested the hypothesis that spontaneous polarization is limited to solid films composed only of molecules of low gas phase dipole moment below 0.7 D. The hypothesis was found to be incorrect. Films of the species methyl[29] and ethyl formate[30] with gas phase dipoles of 1.77 D for *cis*-methyl formate and 1.81 D and 1.98 D for *gauche* and *trans*-ethyl formate respectively and tetrahydrofuran with a dipole of 1.63 D all show spontaneous polarization. It turns out however that the effective dipole moment in the solid state for methyl formate is very likely greatly reduced by a factor of $\sim$ 5 to 0.35 D by the depolarization[22,23] mentioned in section 5. Thus the simple concept, suggested in section 5, of the competition between the grip of effective field at the substrate surface and the tendency of dipoles to align plus to minus may survive these recent observations. Again, only sophisticated calculations can clarify this. In addition the three species of high dipole moment mentioned show hydrogen bonding. This demonstrates that terms associated with hydrogen bonding in the long range pairwise interaction potential, which presumably compete with dipole–dipole in establishing the solid state geometry, do not necessarily preclude spontaneous polarization in solid films. However water ice, with a dipole of 1.85 D, shows no dipole alignment.[12] In water ice, be it amorphous or crystalline, 3D hydrogen bonding is well-known to dictate the structure of the material.

The spontaneous molecular self-organisation described here may have a number of practical applications. For example polarized materials may be used with masking to produce surfaces patterned with potentials, of general application in the field of nanoxerography. Voltage patterned surfaces could for example be employed to create very high density biosensor arrays. In this connection with the future exploration of a range of species it is quite likely that cryo-techniques may be unnecessary. This may be achievable for example by the inclusion of species with longer aliphatic side-chains, noting that dodecyl formate has a melting point of 294.5 K.

Future work will include structural investigations involving X-ray and neutron scattering studies and investigations into the optical properties of these films.

Acknowledgements

We gratefully acknowledge the help of H. C. Fogedby and A. Svane (Aarhus University) in formulating the theory presented here. We also acknowledge support of the staff of the Aarhus Synchrotron Radiation Laboratory (ISA), the Danish Research Council, the LASSIE FP7 ITN network, grant number 238258, a Marie Curie Intra-European Fellowship 009786 (RB) and the Lundbeck Foundation (RB).

References

1 R. Balog, P. Cicman, N. C. Jones and D. Field, *Phys. Rev. Lett.*, 2009, **102**, 073003.
2 F. Jona and G. Shirane, *Ferroelectric Crystals*, Dover Publications Inc., New York, 1993.
3 S. T. Lagerwall, *Ferroelectric and Antiferroelectric Liquid Crystals*, Wiley-VCH, Weinheim, 1999.
4 P. I. C. Teixeira, J. M. Tavares and M. M. Telo da Gama, *J. Phys.: Condens. Matter*, 2000, **12**, R411.
5 R. Moro, X. Xu, S. Yin and W. A. De Heer, *Science*, 2003, **300**, 1265; S. Heiles, J. A. Becker and R. Schäfer, *J. Chem. Phys.*, 2008, **129**, 044304–1.
6 M. Jazniek, I. Mutter and P. Günter, *IEEE J. Sel. Top. Quantum Electron.*, 2008, **14**, 1298 and references therein.
7 E. Ito, *et al.*, *J. Appl. Phys.*, 2002, **92**(12), 7306.
8 O. M. Ottinger, C. Melzer and H. von Seegern, *J. Appl. Phys.*, 2009, **106**, 023704–1.
9 G. McElhinney and J. Pritchard, *Surf. Sci.*, 1976, **60**, 397.
10 K. Radler and J. Berkowitz, *J. Chem. Phys.*, 1979, **70**, 221.
11 S. V. Hoffmann, S. L. Lunt, N. C. Jones, D. Field and J. P. Ziesel, *Rev. Sci. Instrum.*, 2002, **73**, 4157.
12 R. Balog, P. Cicman, D. Field, L. Feketeová, K. Hoydalsvik, N. C. Jones, T. A. Field and J. P. Ziesel, *J. Phys. Chem. A*, 2011, **115**, 6820.
13 B. E. Kohl and C. Panja, *Numerical data and functional relationships in science and technology. Group III, Condensed Matter*, Landolt-Börnstein, Springer, Heidelberg, 2006.
14 M. Michaud, E. M. Hébert, P. Cloutier and L. Sanche, *J. Appl. Phys.*, 2006, **100**, 073705–1.
15 A. Stamatovic and G. J. Schultz, *Rev. Sci. Instrum.*, 1970, **41**, 423.
16 J. Matuska, D. Kubata and S. Matejcik, *Meas. Sci. Technol.*, 2009, **20**, 015901.
17 D. L. Pulfrey, *J. Phys. D: Appl. Phys.*, 1972, **5**, 647; X. Zhou, *et al.*, *Appl. Phys. Lett.*, 2009, **94**, 162901.
18 R. Namann and L. Sanche, *Chem. Rev.*, 2007, **107**, 155.
19 R. M. Marsolais, M. Deschênes and L. Sanche, *Rev. Sci. Instrum.*, 1989, **60**, 2724.
20 K. Zhang and P. Charbonneau, 2011, arXiv:1102.1405v1 [cond-mat.stat-mech].
21 M. E. Lines and A. M. Glass, *Principles and Applications of Ferroelectrics and Related Materials*, Oxford Classic Texts in the Physical Sciences, 2001.
22 A. Natan, L. Kronik, H. Haick and R. T. Tung, *Adv. Mater.*, 2007, **19**, 4103.
23 J. Topping, *Proc. R. Soc. London, Ser. A*, 1927, **114**, 67.
24 S. Homlström and S. Holloway, *Surf. Sci.*, 1986, **173**, L647.
25 E. Cohen de Lara and J. Vincent-Geisse, *J. Phys. Chem.*, 1976, **80**, 1922.
26 B. L. Maschhoff and J. P. Cowin, *J. Chem. Phys.*, 1994, **101**, 8138.
27 D. Fernandez-Torre, O. Kupiainen, P. Pyykkö and L. Halonen, *Chem. Phys.Lett.*, 2009, **471**, 239.
28 D. Field and M. D. Gray, *Mon. Not. Roy. Astr. Soc.*, 1988, **234**, 353.
29 A. Bauder, *J. Phys. Chem. Ref. Data*, 1979, **8**, 583.
30 J. M. Riveros and E. B. Wilson Jr., *J. Chem. Phys.*, 1967, **46**, 4605.